Climatological Relationships between Tropical Cyclones and Rainfall

RANDALL S. CERVENY AND LYNN E. NEWMAN

Department of Geography, Arizona State University, Tempe, Arizona

(Manuscript received 26 March 1999, in final form 24 January 2000)

ABSTRACT

Flooding from tropical cyclone (TC) precipitation has lead in recent years to massive death and loss of property. The identification of climatological linkages between rainfall and TC parameters through study of long-term records would be useful in (i) identifying seasonal predictive climatic parameters to TC development, (ii) producing better precipitation estimates for affected areas, and (iii) developing better parameterizations between storm intensity, latent heat release, and rainfall in hurricane models. This study uses a daily satellite-derived oceanic precipitation record from 1979 to 1995 to determine the rainfall associated with the Atlantic and North Pacific basins over that time period (877 TCs). These data, categorized into 2.5° × 2.5° ocean grid cells, were used to create two precipitation databases. The first uses the surrounding nine grid cells marked from the average position of the tropical cyclone on the day of observation, while the second uses only the center grid cell for the day (representative of only the inner-core precipitation). Strong relationships were found to exist between daily rainfall accumulation and a TC's daily maximum surface wind speeds. The precipitation associated with the inner core is generally representative of the cyclone's total rainfall. The relationship between the ratio of inner-core rainfall and the total storm rainfall with maximum surface winds demonstrates a U-shaped pattern. The inner-core precipitation accounts for nearly 35% of the total rain of the weakest TCs and also of the strongest hurricanes but less than 25% of the total rainfall for weak hurricanes. Forecasters can used rainfall relationships such as these to aid in heavy rainfall and flooding warnings for affected land areas.

1. Introduction

The importance of precipitation in hurricane forecasting was emphasized when Hurricane Mitch caused at least 11 000 deaths through flash flooding and landslides as it devastated Central America in October 1998. Remotely sensed precipitation rates of tropical cyclones (TCs) have long been collected via microwave satellite data (Adler and Rodgers 1977; MacArthur 1991; Schwartz et al. 1994; Schwartz et al. 1996; Wilheit et al. 1982; Wood 1994). Such data have then been incorporated as initial data into, and evaluated in comparison to, numerical simulations of tropical cyclones (e.g., Karyampudi et al. 1995; Krishnamurti et al. 1993; Panegrossi et al. 1998; Shi et al. 1996). However, most past studies focus on specific case studies such that long-term climatological linkages between precipitation and TC parameters have not been investigated in depth. Only a few analyses using a limited number of tropical cyclones (<22 TCs) have studied long-term observed relationships between precipitation and TC wind strength, a cyclone's inner core, or its spatial coordinates (e.g., Rao and MacArthur 1994; Rodgers and Adler 1981). For example, are there linear relationships between precipitation and surface winds? Or does the precipitation of the inner core influence the total precipitation of the system? This study uses a much more extensive observational catalog of tropical cyclones ($n = 877$) from 1979 to 1995.

Such analyses could potentially be useful in (i) identifying seasonal predictive climatic parameters to TC development, (ii) producing better precipitation estimates and forecasts for affected areas, and (iii) developing better parameterizations between storm intensity, latent heat release, and precipitation in hurricane models. Consequently, this study uses a satellite-derived daily oceanic precipitation dataset, together with hurricane and tropical storm observations, to construct climatological relationships between precipitation and commonly determined variables associated with tropical cyclones.

2. Data

The scarcity of long-term empirical precipitation/tropical cyclone intensity relationships has been due in part to the lack of high quality, long-term precipitation records. A long-term dally satellite precipitation record derived from a series of well-calibrated microwave radiometers now exists for the world's oceans. Oceanic

Corresponding author address: Randall S. Cerveny, Department of Geography/Office of Climatology, Arizona State University, Tempe, AZ 85287-0104.
E-mail: cerveny@asu.edu

precipitation estimates (in mm per day over each grid cell) are available using Microwave Sounding Unit (MSU) channels 1 (50.3 GHz), 2 (53.74 GHz), and 3 (54.96 GHz) as gathered by seven separate Television Infrared Observation Satellite-N satellites (Spencer 1993) for the period 1 January 1979 to 31 March 1995. The MSU footprint spatial resolution ranges from 110 km at nadir to over 200 km at the limb. During a large portion of the satellite record (>7.8 years), two-satellite coverage gave both ''morning'' (0730 and 1930 local equator crossing times) and ''afternoon'' (0230 and 1430) information (Spencer 1993). However, Spencer states ''that time series of global rainfall anomalies . . . show no discontinuities during the transitions between one- and two-satellite operations'' (Spencer 1993).

The calibration and intercalibration of the MSUs is described in Spencer et al. (1990) and Spencer (1993), while the rainfall algorithm, discussed by Spencer (1993) is based upon the following relationship:

$$P = aS(\Delta T_{b1})(bT_{air} + c), \quad (1)$$

where P is rainfall in millimeters per day; $a = 3.6$ mm day^{-1} °C^{-1} provides an average match to the monthly rain gauge totals in his Fig. 4 (when averaged over one month, including all zero rain amounts in the average); ΔT_{b1} is channel 1 warming (°C) about a 15% cumulative frequency distribution threshold; and $b = 0.0067$ k^{-1}, $c = -0.83$, and T_{air} (K) provide the necessary correction for the observed latitudinal bias Eq. (1) produces without the temperature correction term. The term T_{air} is a 17-yr average of limb-corrected T_{air} on the 2.5° grid and pentad time resolution. As Spencer (1993) noted, the choice of a climatological average for T_{air} avoids potential cross talk between interannual temperature variations into the precipitation estimates.

These data are categorized into 2.5° × 2.5° ocean grid cells from 60°N to 60°S. The dataset has been used to compare satellite-derived precipitation rates with precipitation rates from 132 island rain gauges (Spencer 1993). A single scale factor, combined with a climatological air temperature dependence term, provided a good match to gauge amounts. This dataset has also been used to identify weekly cycles in precipitation along the eastern North American seacoast (Cerveny and Balling 1998).

Tropical cyclone data are obtained from the National Oceanic and Atmospheric Administration's National Climate Dynamics Center tropical cyclone database (Jarvinen et al. 1984) and, for this study, have been limited to the same time period as the satellite precipitation database (1979–95). Additionally, the quantity (and relative quality) of observations in the Indian and South Pacific basins is somewhat less than their North Pacific and Atlantic basin counterparts so we have limited study to the North Pacific and Atlantic basins. Consequently, from a total of 877 tropical cyclones, a total of 5775 daily observations of tropical cyclones were used in this study.

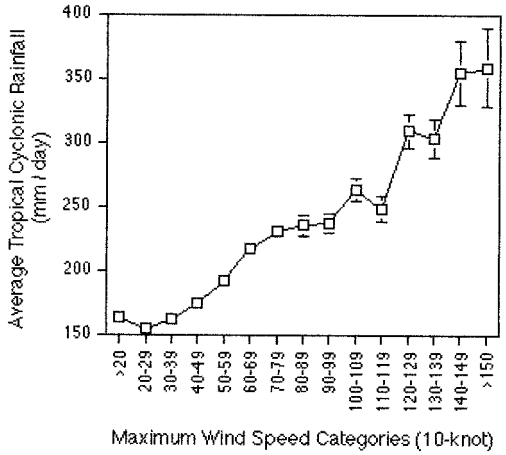

FIG. 1. Relationship between the average tropical cyclonic rainfall (mm day^{-1}) over the nine 2.5° × 2.5° grid cells and the maximum surface wind speed (in 10-kt categories) for tropical cyclonic observations of the Atlantic and North Pacific basins.

Two precipitation databases were formulated. The first was created using the combined rainfall from the surrounding nine grid cells (roughly 220 000 km^2, depending on latitude) marked from the average position of the tropical cyclone on the day of observation. The second dataset uses only the grid cell (approximately 24 000 km^2) in which the average position of the tropical cyclone falls during the given day of observation, consequently restricting precipitation estimates to primarily that of the inner core. Although the geographic size of tropical cyclones can vary greatly, for example, Typhoon Tip versus Tropical Cyclone Tracy (Dunnavan and Diercks 1980; Bureau of Meteorology 1977), as does the translation speed of these storms, the large number of tropical cyclones (877) in our database mitigates these effects to some extent. However, caution is urged if applying our findings to individual tropical cyclones.

3. Results

a. Tropical cyclone perspective

For the combined Atlantic and Pacific basin observations, a highly significant linear relationship exists between the daily amount of TC precipitation accumulated in the nine grid cells and the daily maximum wind speed of the tropical cyclones. Although the mount of variance (r^2) explained between the raw precipitation estimates and wind speed datasets was only 0.12, a better representation of the relationship is obtained when the TC observations are categorized into 10-kt (5.15 m s^{-1}) classes and the mean of each class is used in a regression analysis (Fig. 1). Such a regression analysis yields an explained variance for the combined Atlantic and North Pacific basins of 0.937 ($F = 218$; $p \leq 0.0001$). The regression equation indicates that for every 10-kt (5.15 m s^{-1}) increase in wind speed, there is an

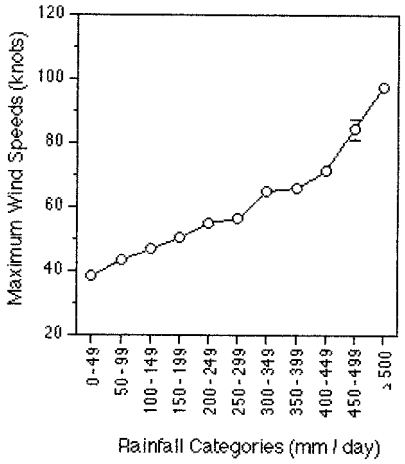

FIG. 2. Relationship between the maximum surface wind speed and the average tropical cyclone rainfall (in 50 mm day^{-1} categories) over the nine grid cells for tropical cyclonic observations of the Atlantic and North Pacific basins.

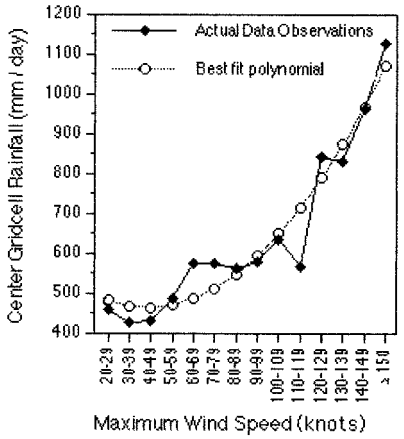

FIG. 3. Relationship between maximum surface wind speed (in 10-kt categories) and center grid cell (inner core) rainfall (mm day^{-1}) of the Atlantic and North Pacific basins. Observed values (solid line); fitted curve (dotted line).

approximately 13 mm day^{-1} increase in TC precipitation. Low wind speed categories (less than 40 kt, 20.6 m s^{-1}) are associated with rainfall amounts of 160 mm day^{-1} while high wind speed categories are characterized by precipitation amounts in excess of 350 mm day^{-1}. Previous studies for much smaller datasets (21 or less typhoons) or for tropical cyclone case studies (e.g., Alliss et al. 1993, 1992; Rao and MacArthur 1994) have demonstrated similar relationships. For example, Allis et al. (1993) found a strong linear relationship between Special Sensor Microwave/Imager rain rates and Hurricane Florence's intensity while Rodgers and Adler (1981) demonstrate a linear relationship between storm intensity and maximum surface winds for 21 typhoons during the early 1970s.

Similarly, when we divide total TC rainfall into 50 mm day^{-1} categories, we find that the reverse relationship also holds; the higher the amount of precipitation associated with the tropical cyclone, the greater the storm wind speed associated with that precipitation (Fig. 2). As with the initial relationship, this reverse regression equation again shows a very high explained variance of 0.940 ($F = 189.9$; $p \leq 0.0001$ level). Low rainfall categories (<300 mm day^{-1}) are characterized by TC wind speeds of less than 60 kt (30.9 m s^{-1}) while high precipitation categories (above 300 mm) are linked to wind speeds of 60 kt (30.9 m s^{-1}) and above. Of course this relationship, as with all others discussed in this study, is climatic in nature and may not be valid for individual storms. For example, Schubert and Hack (1982) have demonstrated that, for individual tropical cyclones, the relationship between maximum surface winds and inner-core rainfall may be nonlinear due to differences in response time to changes in inertial stability.

Another analysis was performed to investigate how representative the rainfall total for the center cell (roughly representative of the inner-core precipitation) is to the average value obtained for the nine-cell domain of the whole tropical cyclone. Approximately 70% of the variance in the average rainfall within the nine-cell area can be explained by the precipitation measured in the center cell. Consequently, it is apparent that the total rainfall of the storm appears to be highly related to the strength of the inner core. To further analyze this effect, the center cell's wind–precipitation relationship was also explored using the aforementioned technique that was applied to the nine–grid cell average rainfall rate. A linear regression fit produced an r^2 value of 0.751 ($F = 39.2$, $p < 0.0001$). However, the results (Fig. 3) show that the data are best represented by a quadratic fit with a regression coefficient of variation r^2 value of 0.925 ($F = 74.0$; $p < 0.0001$). Taking into account this nonlinearity, there is a strong relationship between the nine-cell precipitation average and that measured for the center cell only (Fig. 4). The center cell rainfall explains 98.3% of the variance in the nine-cell rainfall average ($F = 538.6$; $p \leq 0.0001$). This is similar to findings of Rodgers and Adler (1981) for 21 typhoons that occurred in early 1970s. They reported that ''as a tropical cyclone intensifies the rain rate at all distances from the center of circulation increases.''

In terms of the actual rainfall amount, the center grid cell's precipitation contributes 26.3% ± 0.2% of the total rainfall associated with the entire tropical cyclone. When the ratio of the center grid cell precipitation to the TC's entire rainfall is categorized by the storm's wind speed, an interesting U-shaped pattern is evident as illustrated in Fig. 5. More of the TC rainfall is associated with the center grid cell (inner core) precipitation for both very weak storms (those with central wind speeds under 30 kt, 15.4 m s^{-1}) and strong storms (those with central wind speeds above 120 kt, 61.8 m s^{-1}).

The immediate cause of such a relationship is evident

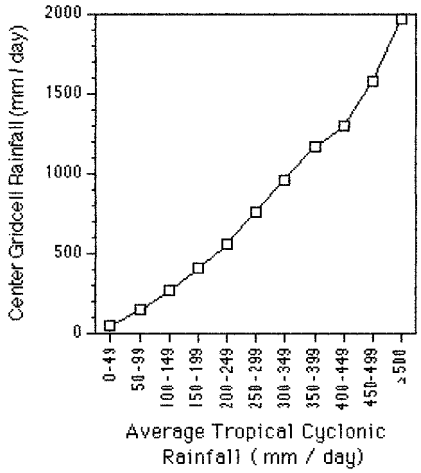

FIG. 4. Relationship between the average tropical cyclone rainfall (50 mm day^{-1} categories) and the center grid cell (inner core) rainfall (mm day^{-1}).

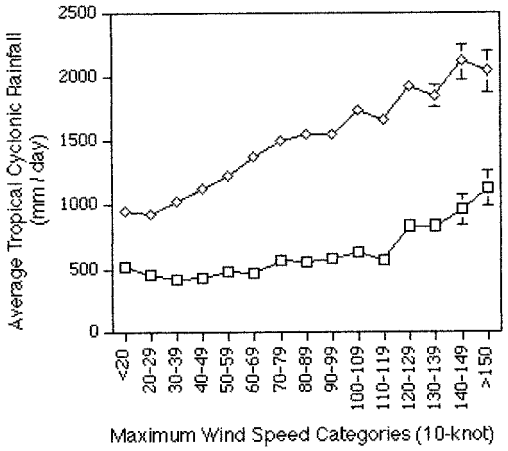

FIG. 6. Center grid cell (inner core) rainfall (squares) and outer grid cells (spiral band) rainfall (diamonds) stratified by maximum surface wind speed (10-kt categories). Bars indicate one standard error deviation about the mean.

when the inner-core and spiral band rainfall is graphed as a function of maximum surface wind speed (Fig. 6). Inner-core precipitation remains relatively constant around 500–600 mm day^{-1} until winds of 120 kt are achieved while spiral band rainfall increases more linearly with increasing surface winds. This suggests that inner-core dynamics, particularly with respect to precipitation, may respond differently than in the outer spiral bands. As addressed earlier, Schubert and Hack (1982), for example, have demonstrated that, for individual tropical cyclones, the relationship between maximum surface winds and inner-core rainfall may be nonlinear due to differences in response time to changes in inertial stability. And, from a theoretical approach, Emanuel (1997) demonstrated while the surface wind field in the inner core can be amplified from wind-induced surface heat exchange, it can also be influenced by the diffusive processes associated with frontal collapse of the eyewall, presumably leading to nonlinear responses with precipitation.

b. Geographical perspective

Analyzing the data from a geographical perspective, the latitudinal gradient of TC precipitation for the combined Atlantic and North Pacific basins is quite steep, as one would expect, with most rainfall of tropical cyclones occurring near the equator (Fig. 7). A marked rapid drop in TC rainfall near the equator is likely the result of the inability to sustain strong TC activity near the equator due to the lack of the Coriolis effect (Anthes 1982). When stratified by basin, the North Pacific west (west of 180°) basin exhibits the pattern closest to the expected relationship (Fig. 8). The North Pacific east (east of 180°) basin shows a marked decline in rainfall

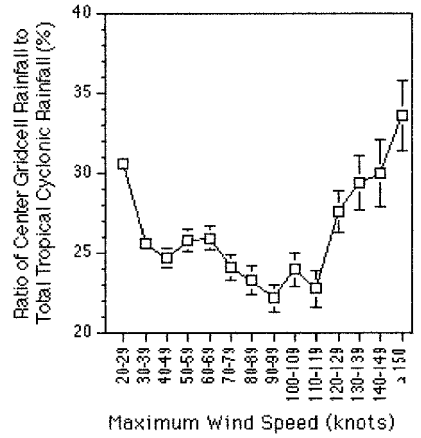

FIG. 5. Ratio of the center grid cell rainfall to the average tropical cyclonic rainfall (in percent) stratified by maximum surface wind speed (10-kt categories). Bars indicate one standard error deviation about the mean.

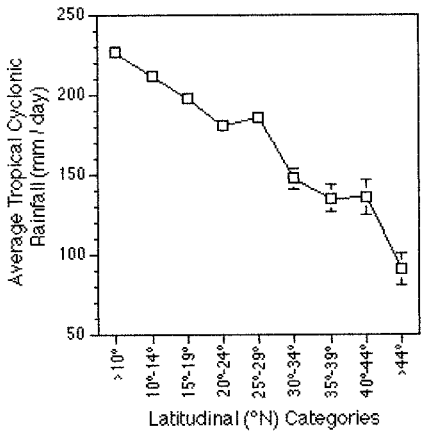

FIG. 7. Latitudinal gradient in average tropical cyclonic rainfall (mm day^{-1}) associated with the North Pacific and Atlantic basins. Bars indicate one standard error deviation about the mean.

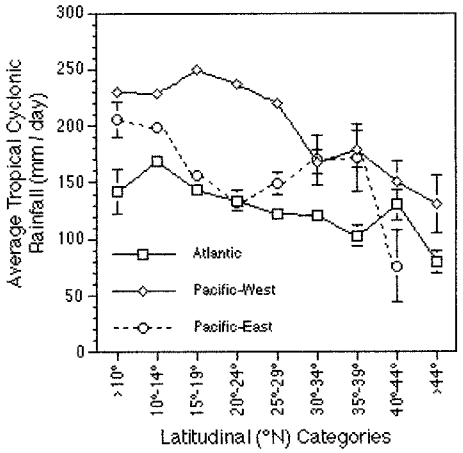

FIG. 8. Latitudinal gradient in average tropical cyclonic rainfall (mm day^{-1}) stratified by basin. (a) Atlantic, squares; (b) North Pacific west, diamonds; (c) North Pacific east, circles with dashed lines. Bars indicate one standard error deviation about the mean.

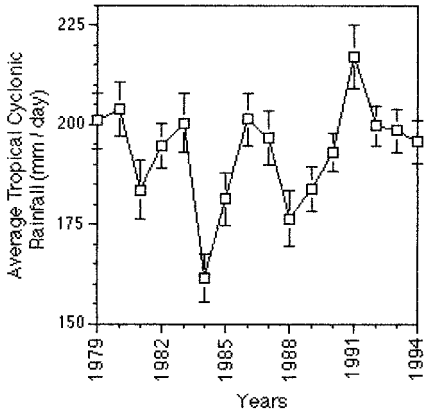

FIG. 10. Average tropical cyclonic rainfall (mm day^{-1}) for the combined North Pacific and Atlantic basins by year.

as latitude increases until approximately 25°N, when precipitation again increases as storms approach higher latitudes (north to about 35°N). The drop in precipitation likely results from a weakening of the tropical cyclone as the storm enters the colder waters off the coast of North America. The Atlantic basin also deviates from the expected pattern with low rainfall rates at low latitudes (although there are relatively few Atlantic storms in the 0°–10°N range) and high rainfall in the 10°–15°N range with dropping rates into the midlatitudes. Around 40°–45°N there is a significant increase in precipitation followed by an equally marked decrease in the rainfall rate as storms continue moving poleward, perhaps due to a variety of extratropical influences (Tuleya 1994) such as the effects of the Gulf Stream, interactions with extratropical weather features (e.g., Drury and Evans 1998), or penetration into a high pressure ridge's subsidence.

The North Pacific and Atlantic tropical cyclones occurring during the months of October, November, December, and January experience significantly more rain per day than do storms throughout the rest of the year (Fig. 9). In other words, the later season TCs appear to be wetter than early season storms. The North Pacific east basin's November and December tropical cyclones, in particular, tend to be heavy rain producers. The explanation for this finding relates to the relationship between wind speeds and rainfall in conjunction with the timing of most intense tropical cyclones, particularly for the North Pacific basins. Although analysis of the TC dataset reveals that, for the North Atlantic basin, the timing of the most intense tropical cyclones occurs in early September, the most intense tropical cyclones in the North Pacific Ocean basins occur much later in the year (November and December). Because these late season storms generally are occurring in low latitudes, they are drawing on the warmer temperatures, moisture, and surface energies available at those latitudes. As example of this behavior, Supertyphoon Paka with sustained

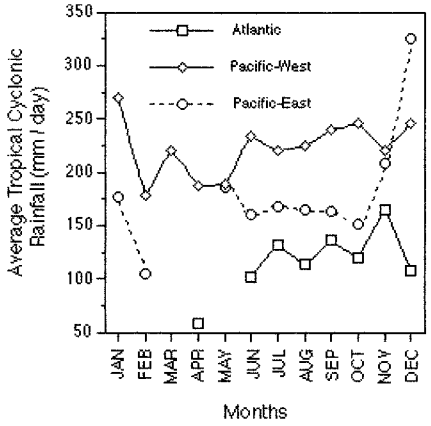

FIG. 9. Monthly variations in average tropical cyclonic rainfall (mm day^{-1}) stratified by basin. (a) Atlantic, squares; (b) North Pacific west, diamonds; (c) North Pacific east, circles with dashed lines. Bars indicate one standard error deviation about the mean.

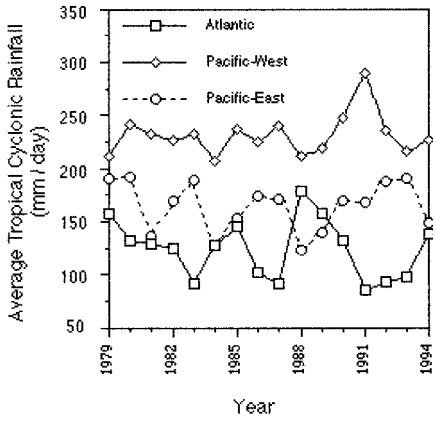

FIG. 11. Average tropical cyclonic rainfall (mm day^{-1}) stratified by basin and year. (a) Atlantic, squares; (b) North Pacific west, diamonds; (c) North Pacific east, circles with dashed lines. Bars indicate one standard error deviation about the mean.

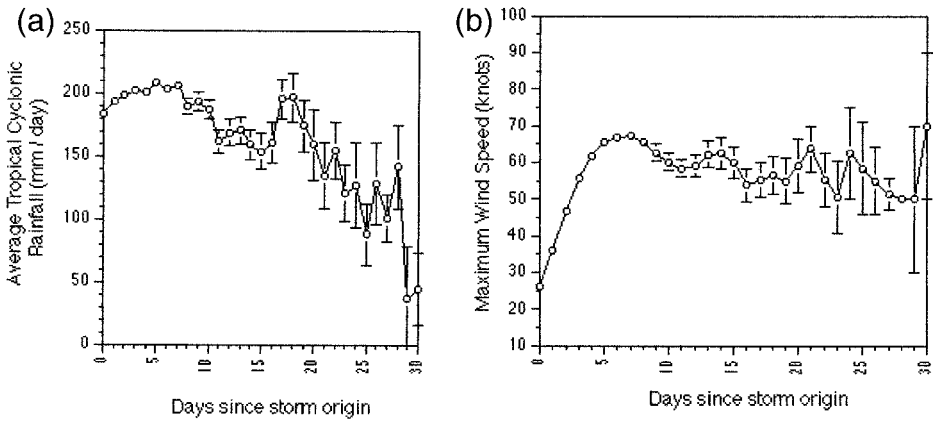

FIG. 12. (a) Average tropical cyclonic rainfall (mm day^{-1}) for the North Pacific and Atlantic basins categorized by the number of days since the origin of the tropical cyclone. (b) Maximum surface wind speed (kt) associated with tropical cyclones in the North Pacific and Atlantic basins as categorized by the number of days since the origin of the tropical cyclone. Bars indicate one standard error deviation about the mean.

winds of 175 kt hit Guam late in the year on 17 December 1997. Given the primary finding of this study of a strong linear relationship between wind speed and rainfall, it is consequently not surprising that TC precipitation is higher toward the end of the year.

Although too short of record exists to identify substantially strong temporal cycles in the tropical cyclone precipitation database, marked ''dry'' tropical cyclone years have occurred in 1981, 1984–85, and 1988–89. Strong ''wet'' tropical cyclone years have occurred in 1979–80, 1982–83, 1986–87, and 1991 (Fig. 10). As expected, the North Pacific and Atlantic tropical cyclone rainfall rates are out of phase with each other over time (Fig. 11). This relationship appears to follow the variance identified between the North Pacific and Atlantic basins with regard to El Niño events (Gray 1984). In the Atlantic basin during El Niño events, increased vertical shear brought about by increases in the climatological westerly winds in the upper troposphere result in few TCs (Gray 1984; Pielke and Landsea 1999). Conversely, records of past El Niño events indicate that such events produce consistently warmer than normal sea surface temperatures in the Pacific, especially near the international date line, and consequently more typhoons (Chan 1985; Chu and Clark 1999; Chu and Wang 1997).

Rainfall as a function of a tropical cyclone's lifetime tends to demonstrate a peak in rainfall for the combined Atlantic and North Pacific basins at approximately six days (Fig. 12a). Maximum daily wind speed as a function of the number of days since the origin of the storm shows a marked increase in velocity with a peak around 6–7 days (Fig. 12b). Separating this analysis by basin, the North Pacific west basin is the ocean basin primarily driving this behavior. A quasi-''weekly'' behavior in TC rainfall or winds is likely linked to the average lifetime of the storm. For the 877 tropical cyclones analyzed in this study, the average lifetime of a tropical cyclone was 8 days (with a secondary peak at 6 days). Statistically, the maximum wind speeds, which tend to occur near the middle of the TC's life cycle, tend to peak near the same time period. The close relationship between wind maxima and rainfall indicates that rainfall will consequently follow the same pattern.

4. Discussion and conclusions

The climatology of rainfall rates associated with tropical cyclone activity shows clear linear relationships between the intensity of the tropical activity and the amount of precipitation for the North Pacific and Atlantic basins.

- When the TC wind observations are categorized into 10-kt (5.15 m s^{-1}) classes and the mean of each class is used in the analysis, the resulting linear regression of maximum surface wind classes explained 94% of the total variance in precipitation ($p < 0.0001$). Previous studies for much smaller datasets and TC case studies have demonstrated similar relationships.
- The reverse relationship is equally valid, which adds support to the linkage. The higher the TC rainfall category, the greater the maximum surface wind speed associated with the precipitation class. The total rainfall of the tropical cyclone appears to be highly related to the precipitation associated with the inner core. Approximately 70% of the variance in the total rainfall within the nine-cell area can be explained by the precipitation measured in the center grid cell ($F = 41.0$; $p < 0.0001$). This is empirical evidence that the mechanisms associated with the TC's inner core directly influence the release of rainfall in its spiral bands. Our findings probably relate to the concepts associated with development of spiral rain bands from the center. Although there has been disagreement as to whether

the spiral bands are created by gravity waves (Willoughby 1978), boundary layer asymmetry (Shapiro 1983), or pooled potential vorticity regions (Gunn and Schubert 1993), it is nevertheless very likely that energy is exchanged between the inner core and the system's spiral bands, and that the two features are related. As Rodgers and Adler (1981) reported, ''as a tropical cyclone intensifies the rain rate at all distances from the center of circulation increases.''

- A larger portion of the TC's total precipitation is associated with the center box (inner core) precipitation for both very weak storms (those with central wind speeds under 30 kt, 15.4 m s^{-1}) and strong storms (those with central wind speeds above 120 kt, 61.8 m s^{-1}). This is the result of the fact that inner-core precipitation remains relatively constant around 500–600 mm day^{-1} until winds of 120 kt are achieved while spiral band rainfall increases more linearly with increasing surface winds. The implication, as suggested from previous case studies, is that inner-core dynamics, particularly with respect to precipitation, may respond differently than in the outer spiral bands.
- The latitudinal gradient of precipitation associated with tropical cyclones for the combined Atlantic and North Pacific basins is steep with most TC rainfall occurring near the equator. The moisture availability associated with the subtropics is likely the factor behind this finding.
- Although past studies have indicated that TC frequencies are highest in September, tropical cyclones that occur in the months of October, November, December, and January produce significantly more precipitation per day than do other months of the year. This is likely associated with the timing of the most intense tropical cyclones that for North Pacific Ocean basins occur late in the year (November and December). The geographic and temporal findings suggest that late-season storms, particularly in the North Pacific basin, are more low latitude than their summer counterparts and, consequently, they are drawing on the warmer temperatures, moisture, and surface energies available at those latitudes.
- As expected, the North Pacific and Atlantic TC rainfall rates are out of phase with each other over the length of record (1979–95) in accordance with El Niño–La Niña relationships. Given that past studies (e.g., Gray 1984) have shown that Atlantic TC activity is suppressed under El Niño conditions while Pacific tropical cyclone activity is enhanced due to warmer SSTs (Chan 1985; Chu and Clark 1999; Chu and Wang 1997), it is not surprising to see a decrease in Atlantic TC rainfall and an increase in Pacific TC rainfall occurring under such conditions.
- Rainfall as a function of storm lifetime shows a peak in rainfall for the combined Atlantic and Pacific basins at approximately six days declining until another major peak occurs around 17–18 days. The former peak of 6 days is likely related to the average TC lifetime while the latter peak (17–18 days) may relate to the travel time that some storms would take that have crossed the Atlantic and then reached the warmer waters of the Gulf Stream. Similarly, in the Pacific, storms would traverse the basin and then enter the warmer waters associated with the Kuroshio Current.

These results demonstrate basic associations between satellite-derived precipitation and measures of TC intensity. One application of these results is the production of better rainfall rates for areas affected by tropical cyclones. For example, as Fig. 1 demonstrates, a minimal strength hurricane (winds of 60 kt, 61.8 m s^{-1}) produces rains on the order of 225 mm day^{-1} over the nine grid cells of 2.5° × 2.5° size. That can be converted to approximately 41 million acre-feet of rain per day for the entire area of the tropical cyclone. Conversely, a storm of wind strength greater than 100 kt (51.5 m s^{-1}) produces approximately 120 million acre-feet of rain per day over an area of 220 000 km^2. This magnitude of precipitation is the equivalent of filling Lake Erie (391 987 200 acre-feet) in three and one-quarter days. In terms of manmade structures, one of the largest, Hoover Dam with a capacity of approximately 28 million acre-feet, could be filled by even a minimal hurricane in just over half a day. Such statistics demonstrate the tremendous amount of water available for flooding such as in the tragedy associated with Hurricane Mitch (1998).

Rainfall estimates like these can be used by forecasters as climatological averages to aid in heavy rainfall and flooding warnings for affected land areas. Continued study of these relationships can improve and aid our theoretical and applied understanding of tropical cyclonic rainfall.

Acknowledgments. We deeply thank Dr. Chris Landsea and two anonymous reviewers for their valuable comments on this paper.

REFERENCES

Adler, R. F., and E. B. Rodgers. 1977: Satellite-observed latent heat release in tropical cyclones. *Mon. Wea. Rev.,* **105,** 956–963.

Alliss, R. L., S. Raman, and S. W. Chang, 1992: Special Sensor Microwave/Imager (SSM/I) observations of Hurricane Hugo (1989). *Mon. Wea. Rev.,* **120,** 2723–2737.

——, G. D. Sandlin, S. W. Chang, and S. Raman, 1993: Applications of SSM/I data in the analysis of Hurricane Florence (1988). *J. Appl. Meteor.,* **32,** 1581–1591.

Anthes, R. A., 1982: *Tropical Cyclones: Their Evolution, Structure and Effects. Meteor. Monogr.,* No. 19, Amer. Meteor. Soc., 208 pp.

Australian Bureau of Meteorology, 1977: Report by Director of Meteorology on Cyclone Tracy, December 1974. Australian Bureau of Meteorology, Melbourne, Australia, 82 pp.

Cerveny, R. S., and R. C. Balling Jr., 1998: Weekly cycles of air pollutants, precipitation and tropical cyclones in the coastal NW Atlantic region. *Nature,* **394,** 561–563.

Chan, J. C. L., 1985: Tropical cyclone activity in the Northwest Pacific in relation to the El Niño/Southern Oscillation phenomenon. *Mon. Wea. Rev.,* **113,** 599–606.

Chu, P.-S., and J. Wang, 1997: Tropical cyclone occurrences in the vicinity of Hawaii: Are the differences between El Niño and Non-El Niño years significant? *J. Climate*, **10,** 2683–2689.

——, and J. D. Clark, 1999: Decadal variations of tropical cyclone activity over the central North Pacific. *Bull. Amer. Meteor. Soc.*, **80,** 1875–1881.

Drury, S., and J. L. Evans, 1998: Modeling of tropical cyclone intensification as a result of interaction with midlatitude troughs. Preprints, *Symp. Tropical Cyclone Intensity Change*, Phoenix, AZ, Amer. Meteor. Soc., 65–72.

Dunnavan, G. M., and J. W. Diercks, 1980: An analysis of Supertyphoon Tip (October 1979). *Mon. Wea. Rev.*, **108,** 1915–1923.

Emanuel, K. A., 1997: Some aspects of hurricane inner-core dynamics and energetics. *J. Atmos. Sci.*, **54,** 1014–1026.

Gray, W. H., 1984: Atlantic seasonal hurricane frequency. Part I: El Niño and 30 mb quasi-biennial oscillation influences. *Mon. Wea. Rev.*, **112,** 1649–1668.

Gunn, T. A., and W. H. Schubert, 1993: Hurricane spiral bands. *J. Atmos. Sci.*, **50,** 3380–3403.

Jarvinen, B. R., C. J. Neumann, and M. A. S. Davis, 1984: A tropical cyclone data tape for the North Atlantic basin, 1886–1983: Contents, limitations, and uses. NOAA Tech. Memo. NWS NHC 22, 21 pp.

Karyampudi, V. M., G. Lai, J. Monobianco, and S. Koch, 1995: Sensitivity of Hurricane Florence (1988) development to initial conditions, assimilation of satellite-derived rainfall rates and convective parameterization schemes. Preprints, *21st Conf. Hurricanes and Tropical Meteorology*, Miami, FL, Amer. Meteor. Soc., 386–388.

Krishnamurti, T. N., H. S. Bedi, and K. Ingles, 1993: Physical initialization using SSM/I rain rates. *Tellus*, **45A,** 247–269.

MacArthur, P. D., 1991: Microwave derived rain rates in typhoons and their use in the diagnosis and prediction of typhoon intensity. M.S. thesis, Dept. of Earth and Atmospheric Sciences, St. Louis University, 69 pp.

Panegrossi, G., and Coauthors, 1998: Use of cloud model microphysics for passive microwave-based precipitation retrieval: Significance of consistency between model and measurement manifolds. *J. Atmos. Sci.*, **55,** 1644–1673.

Pielke, R. A., Jr., and C. N. Landsea, 1999: La Niña, El Niño and Atlantic Hurricane Damges in the United States. *Bull. Amer. Meteor. Soc.*, **80,** 2027–2033.

Rao, G. V., and P. D. MacArthur, 1994: The SSM/I estimated rainfall amounts of tropical cyclones and their potential in predicting the cyclone intensity changes. *Mon. Wea. Rev.*, **122,** 1568–1574.

Rodgers, E. B., and R. F. Adler, 1981: Tropical cyclone rainfall characteristics as determined from a satellite passive microwave radiometer. *Mon. Wea. Rev.*, **109,** 506–521.

Schubert, W. H., and J. J. Hack, 1982: Inertial stability and tropical cyclone development. *J. Atmos. Sci.*, **39,** 1687–1697.

Schwartz, M. J., J. W. Barrett, P. W. Fieguth, P. W. Rosenkranz, M. S. Spina, and D. H. Staelin, 1994: Passive microwave imagery of a tropical storm near 118 GHz: Thermal and precipitation structure. *Proc. Int. Geoscience Remote Sensing Symp.*, Pasadena, CA, IEEE, 2433–2435.

——, ——, ——, ——, ——, and ——, 1996: Observations of thermal and precipitation structure in a tropical cyclone by means of passive microwave imagery near 118 GHz. *J. Appl. Meteor.*, **35,** 671–678.

Shapiro, L. J., 1983: The asymmetric boundary layer flow under a translating hurricane. *J. Atmos. Sci.*, **40,** 1984–1998.

Shi, J.-J., S. W. Chang, and S. Raman, 1996: Impact of assimilation of dropwindsonde data and SSM/I rain rate on numerical prediction of Hurricane Florence (1988). *Mon. Wea. Rev.*, **124,** 1435–1448.

Spencer, R. W., 1993: Global oceanic precipitation from the MSU during 1979–91 and comparisons to other climatologies. *J. Climate*, **6,** 1301–1326.

——, J. R. Christy, and N. C. Grody, 1990: Global atmospheric temperature monitoring with satellite microwave measurements: Method and results, 1979–84. *J. Climate*, **3,** 1111–1128.

Tuleya, R. E., 1994: Tropical storm development and decay: Sensitivity to surface boundary conditions. *Mon. Wea. Rev.*, **122,** 291–304.

Wilheit, T., and Coauthors, 1982: Microwave radiometric observations near 19.35, 92, and 183 GHz of precipitation in Tropical Storm Cora. *J. Appl. Meteor.*, **21,** 1137–1145.

Willoughby, H. E., 1978: Possible mechanism for the formation of hurricane rainbands. *J. Atmos. Sci.*, **35,** 838–848.

Wood, V. T., 1994: A technique for detecting a tropical cyclone center using a Doppler radar. *J. Atmos. Oceanic Technol.*, **11,** 1207–1216.